

Monte Carlo studies of three-dimensional two-step restricted self-avoiding walks

Ling Heng Wong and Aleksander L Owczarek

Department of Mathematics and Statistics, The University of Melbourne, Vic. 3010, Australia

E-mail: henryw@ms.unimelb.edu.au and aleks@ms.unimelb.edu.au

Received 18 June 2003, in final form 29 July 2003

Published 2 September 2003

Online at stacks.iop.org/JPhysA/36/9635

Abstract

Two-step restricted walk (TSRW) models are a class of restricted self-avoiding walk (SAW) where, in addition to the self-avoidance constraint, certain restrictions are placed upon each pair of successive steps. In this paper, we explore the relationship between the restrictions and the scaling of the average size of walks in three-dimensional models. We use the Pruned-enriched Rosenbluth method algorithm to perform Monte Carlo studies in five representative TSRW models in three dimensions. The results present strong numerical evidence that all non-trivial TSRW models in three dimensions have the same size scaling behaviour as unrestricted SAWs. This is in contrast to two dimensions where several universality classes are accepted to exist. In particular, we find no rule analogous to the ‘spiral’ walk of two dimensions.

PACS numbers: 05.50.+q, 05.10.Ln, 05.40.–a

1. Introduction

The self-avoiding walk (SAW) model has long been used as a standard model for linear polymer behaviour [1–4]. Due to both the difficulties in finding an exact solution to the model [5] and the wish to understand the robustness of the universality class of SAWs, much effort has been directed towards studying modified models. *Two-step restricted walk* (TSRW) models [6, 7] are a class of restricted SAW models—the allowed configurations are oriented walks that have certain restrictions placed upon each pair of successive steps in addition to the self-avoidance constraint. The walk rule of each model can be conveniently depicted by a ‘rule diagram’, denoting the possible next steps after each step—three-dimensional examples can be found in figure 1.

The average (squared) geometric size of the walks, measured by the radius of gyration squared or an eigenvalue of the moment of inertia tensor for example, in any of these models is generally expected to grow asymptotically as

$$\langle R^2 \rangle_N \sim N^{2\nu} \{B_0 + B_1 N^{-\Delta} + B_2 N^{-1} + \dots\} \quad \text{as } N \rightarrow \infty \quad (1)$$

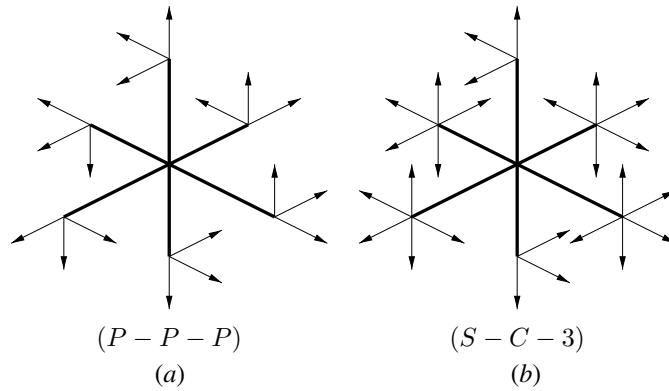


Figure 1. Three-dimensional rule diagrams for (a) model S and (b) model A proposed by Guttmann and Wallace [15]. One specifies which of the next steps (arrowed lines) is allowed from each of the six lattice bonds (full lines) representing the current step of the walk. The three-character code is used in this work as a name—see main text for explanation.

Table 1. Two-dimensional universality classes of TSRW on the square lattice. The number of walks of length N is c_N . The accepted or proved scaling forms of c_N as N becomes large are shown in column two. The next two columns give values of the size exponent ν . There are two values for the exponent ν associated with the scaling of the geometric size of the walks and are related to the major (ν_+) and minor (ν_-) directions of the average moment of inertia tensor for the configurations. For spiral walks, confluent logarithmic factors appear in the asymptotics. The right-most column contains the rules used in this paper for the construction of three-dimensional rules (see table 2).

Universality class	Scaling form for c_N	ν_+	ν_-	Rules
SAW	$c_N \sim C\mu^N N^{\gamma-1}$	$\frac{3}{4}$	$\frac{3}{4}$	S
Spiral	$c_N \sim C e^{\frac{2\pi}{3}\sqrt{N}} N^{\frac{7}{4}}$	$\frac{1}{2}(\log)$	$\frac{1}{2}(\log)$	P
Directed	$c_N \sim C\mu^N$	1	$\frac{1}{2}$	D
Aniso-spiral	$c_N \sim C\mu^N e^{a\sqrt{N}} N^\beta$	0.95(2)	0.47(1)	3 and 2
One-dimensional	$c_N \sim CN$	1	0 or 1	O, R and C
Trivial	$c_N \sim C$	0	0	

where $B_0, B_1, B_2 \dots$ are some real constants and ν is called the *size exponent*; the non-analytic correction-to-scaling exponent $\Delta \in \mathbb{R}^+ \setminus \mathbb{Z}^+$ may be absent if $\langle R^2 \rangle_N$ has only analytic correction-to-scaling terms. Confluent logarithmic factors can also exist in some models.

In this work, we shall consider the full moment of inertia tensor and define the notations ν_+ and ν_- to be the values of the scaling exponent for the maximal and minimal eigenvalues, respectively. For the unrestricted SAW model, $\nu_+ = \nu_- = 3/4$ in two dimensions [8], and $\nu_+ = \nu_- \approx 0.588$ in three dimensions [9–11]. Some of the walk restrictions are known to cause different size scaling¹ from that of the unrestricted model. For instance, $\nu_+ = 1$ and $\nu_- = \frac{1}{2}$ for directed walks in two dimensions [12]. There is a classification [6, 7, 13] of two-dimensional TSRW models delineated according to the values of ν_+ and ν_- , a summary of which is given in table 1. The study of models in the aniso-spiral walk class [14] needs further work as good values of the exponents and a full understanding of that universality class is still lacking.

A central question addressed in [6] was ‘Do properties of these rules determine the universality class?’ There it was suggested that the symmetry of the walk rules in two

¹ Reflected by either a different asymptotic form or a different value of ν .

Table 2. Planar walk rules used in the construction of three-dimensional rules.

<i>S</i>	<i>3</i>	<i>2</i>	<i>P</i>
Unrestricted SAW 	Three-choice walk 	Two-choice walk 	Planar spiral
<i>D</i>	<i>C</i>	<i>O</i>	<i>R</i>
Directed walk 	Concatenations of 1D walks 	One-dimensional 	Rectangular

dimensions, as seen in the rule diagrams, gives insight into which universality class the model falls. In this paper, we investigate if such a relationship exists in three-dimensional TSRW models. The aim of this paper is to investigate the proposed delineation of non-trivial universality classes in three dimensions of TSRW models as suggested in [7] and subsequently to re-evaluate the relationship between the microscopic features (in particular the symmetry) of the walk rule of a model and the university class into which it falls.

Aside from trivial and directed walk models, Guttmann and Wallace [15] were the first to propose non-trivial three-dimensional TSRW models. Their original aim was to find walk rules that create walks that display a ‘spiralling’ property, i.e. those that produce walks which wrap around the origin. Accordingly, they defined model *S* (also known as the three-dimensional spiral walk) and model *A* (also known as the three-dimensional aniso-spiral walk)—associated rule diagrams are depicted in figure 1. Using exact enumeration data, they estimated that the size exponent for model *S* is $\nu = 0.67 \pm 0.10$, which possibly signalled a distinct universality class from the class of unrestricted SAW. On the other hand, the size of the error estimate for model *S* encompasses the unrestricted value. For model *A*, they estimated that $\nu = 0.595 \pm 0.025$, which suggested that that model is in the same class as the unrestricted SAW.

Rechnitzer and Owczarek undertook a systematic study of three-dimensional TSRW models in [7]. In three dimensions, however, the number of distinct TSRW models is $2^{6 \times 5} = 1\,073\,741\,824$, so in order to reduce this set to a manageable size, it was paramount to devise a scheme to eliminate trivial, one-dimensional, or directed walks, which are deemed ‘uninteresting’. They introduced a nomenclature for three-dimensional walk models: each walk model was denoted with a three-letter code (*Z*–*Y*–*X*), where *Z* denotes the planar walk model on the plane normal to the *z*-axis, *Y* denotes the planar walk model on the plane normal to the *y*-axis and similar for *X*. The letters that we shall use in our study are defined in table 2. However, as pointed out in [7] not all possible combinations of three letters create consistent and thus possible walk rules. For instance, (*O*–*O*–*R*) is an impossible rule. Under this system, Guttmann and Wallace’s models *S* and *A* are given the codes (*P*–*P*–*P*) and (*S*–*C*–*3*), respectively.

To eliminate ‘uninteresting’ walk models, two conditions were enforced, namely: (i) symmetric ‘balance’ condition which is a combination of two conditions—balance and reverse-balance conditions and (ii) the mixing condition. The ‘balance’ condition requires that the

walk rule (not any particular configuration though) has equal numbers of continuing steps in the positive and negative components of each axis. Models violating this condition are expected to be biased in a particular direction and so be directed or one-dimensional. The reverse-balance condition is similar to the balance condition except that it concerns the corresponding ‘reverse’ walk rule: that is, considering the rule produced by reversing the orientation of the configurations produced from a particular rule. Indeed, there are walk rules which are balanced that have a reverse rule which is not so (for example rule (k) in [6]). The mixing condition requires that after a step in any one of the six directions (in three dimensions) the walk is able to eventually take a step in any of the six directions. This condition also attempts to exclude directed rules. There are 432, 096 TSRW models in three dimensions that satisfy these conditions [7] and these models are called *symmetric-mixing* models. To further reduce the size of the set under consideration, Rechnitzer and Owczarek [7] enforced another condition that no more than one plane has a one-dimensional or directed rule (e.g., D , C , O or R). They chose nine of the most ‘promising’ models to analyse based on their numerical behaviours [7]. They also chose three other models not constructed in the above manner to have representatives of walk rules with as many symmetries as possible. They computed various exact enumerations for each of the models and used differential approximants [16] to analyse the number of configurations c_N , the radius of gyration series and the eigenvalues series of the mean moment of inertia matrices to give estimates of the size exponents. The differential approximants of these models were found to cluster into three distinct bands, and the central estimates of the exponents differed appreciably from each other, which led them to tentatively suggest that there may be at least three non-trivial universality classes in three dimensions; these possible classes are²

1. SAW: $(S-S-S)$, $(S-C-3)$, $(3-3-C)$, $(S-C-P)$, $(\text{Rot}-\pi)$ and $(S-P-3)$ model;
2. Three-dimensional spiral: $(P-P-P)$ and $(P-R-2)$ models;
3. New: $(P-O-3)$, $(P-3-3)$ and $(P-2-2)$ models; and
4. Undetermined: $(P-P-D)$ and $(P-P-3)$ models.

This classification is consistent with the earlier conclusion by Guttmann and Wallace [15] regarding the $(S-C-3)$ and $(P-P-P)$ models. However, there were several concerns that were discussed in [7]. There appears to be no obvious relationship between the walk rule symmetry and the universality class that they fall into, as opposed to two dimensions, except a possibly relevant new statistic known as the *turning number* [7]. Also, estimates of the systematic error of the differential approximant analysis for size exponent ν overlapped mostly with the unrestricted model, and, finally, estimates of the exponent γ derived from the total number of walks did not display the same banding pattern.

Indeed it was suggested [7] that the delineation of universality class in three dimensions is only due to different degrees of finite-length correction effects across classes, and all non-trivial walk models in fact fall into a single universality class. The systematic error detected in the differential approximant analysis suggests that a different approach should be attempted. Therefore, there is a need to test this universality classification by studying much longer walks using the Monte Carlo methods—the approach we shall pursue here.

2. Simulation details

In total, we have studied five symmetric-mixing walk models (including the unrestricted walk model as a benchmark) which have been previously studied in [7, 15]. They were chosen

² The boxed models are those we shall study in detail in this paper.

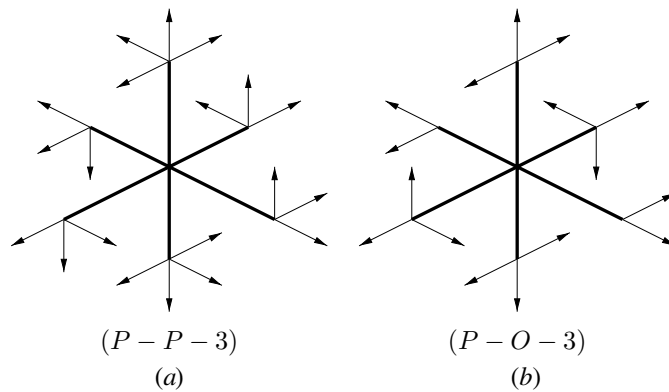


Figure 2. Three-dimensional rule diagrams for the (a) $(P-P-3)$ and (b) $(P-O-3)$ models.

out of the original 12 models in [7] because each of them represented a possible universality class in [7], and they included the unrestricted SAW model and the two models proposed by Guttmann and Wallace [15]. All their rule diagrams can be found in figures 1 and 2, except that of the unrestricted SAW model, which, of course, simply allows all possible continuing steps.

We have chosen the Pruned-enriched Rosenbluth method (PERM) algorithm [17] to simulate walks in all these five symmetric-mixing models. It is because the PERM algorithm is relatively easy to modify to account for the TSRW model restrictions and the demonstrated efficiency of the algorithm for SAW simulations that led us to choose PERM. Other candidate algorithms such as the also efficient *pivot* algorithm [18] are difficult to adapt to TSRW models since the walk rules are very difficult to maintain during the pivoting operations. We have modified the PERM algorithm as given in [19]. We have calculated the *mean moment of inertia tensor* to give a more complete picture of how the walk model scales in three-dimensional space. This measure often provides a more robust estimate of the size exponents than the mean end-to-end distance and mean monomer-to-end distance.

Since long walks are built upon shorter ones in the PERM algorithm, the statistics that we take from various points of a single walk simulated by PERM are correlated. In order to eliminate this correlation problem, we have performed *independent* runs of simulation for *each* walk length N , where $16 \leq N \leq 8,192$ in steps of power two, in each model (except for shorter walks where $N \leq 256$, data were less important with respect to the eventual asymptotic behaviours and hence they were collected from a single run of simulation). Each model consumed roughly 2 months of CPU time on a Compaq DECAalpha (667 MHz). We have generated 50 000 000 samples of walks of length $N = 8192$ in each model.

3. Data and analysis

For each of the symmetric-mixing models, we performed the following analysis. For any given simulated walk, $\omega_N = \{r_i = (x_i, y_i, z_i) : 0 \leq i \leq N\}$ of length N , we measure its geometric size by its *moment of inertia tensor matrix*, $\mathbf{I}(\omega_N)$, which is defined to be

$$\mathbf{I}(\omega_N) = \frac{1}{n+1} \sum_{i=0}^N (r_i^2 \mathbf{1} - r_i r_i) = \frac{1}{n+1} \sum_{i=0}^N \begin{pmatrix} y_i^2 + z_i^2 & -x_i y_i & -x_i z_i \\ -x_i y_i & x_i^2 + z_i^2 & -y_i z_i \\ -x_i z_i & -y_i z_i & x_i^2 + y_i^2 \end{pmatrix} \quad (2)$$

where $\mathbf{1}$ is the identity tensor. The *mean* moment of inertia tensor over all walks of length N is therefore defined to be

$$\langle \mathbf{I} \rangle_N = \frac{1}{c_N} \sum_{\omega_N} \mathbf{I}(\omega_N) \quad (3)$$

where c_N is the number of walks of length N in the model. Diagonalizing $\langle \mathbf{I} \rangle_N$, the eigenvectors correspond to the *natural* coordinate axes in which the walk model scales on average; and the respective eigenvalues correspond to the radius of gyration along those axes—we denote the eigenvalues and their corresponding eigenvectors at length N by $\{\lambda_1(N), \lambda_2(N), \lambda_3(N)\}$ and $\{\mathbf{v}_1, \mathbf{v}_2, \mathbf{v}_3\}$, respectively. Note that \mathbf{v}_i are expected to be independent of N , at least for sufficiently large N . Following what we have discussed earlier, we expect that

$$\lambda_i(N) \sim A_i N^{2\nu_i} \quad i = 1, \dots, 3 \quad \text{as } n \rightarrow \infty. \quad (4)$$

Using the Monte Carlo simulations, we obtained estimates of the mean moment of inertia matrix

$$\langle \hat{\mathbf{I}} \rangle_N \approx \frac{1}{|\mathbf{S}|} \sum_{\omega_N \in \mathbf{S}} \mathbf{I}(\omega_N) \quad (5)$$

where \mathbf{S} is the set of samples generated from the simulations. We have calculated a corresponding *error matrix*, $\delta \mathbf{I}_N$, which contains the estimated error of all entries in $\langle \hat{\mathbf{I}} \rangle_N$.

To estimate $\lambda_i(N)$, we diagonalized $\langle \hat{\mathbf{I}} \rangle_N$ and we denote its i th eigenvalue by $\hat{\lambda}_i(N)$. To estimate the error of $\hat{\lambda}_i(N)$, denoted by $\delta \hat{\lambda}_i(N)$, which results from the errors of the entries in $\langle \hat{\mathbf{I}} \rangle_N$, we used Wilkinson's rigorous bound [20] which showed that

$$|\delta \hat{\lambda}_i(N)| \leq \frac{\|\delta \mathbf{I}_N\|_2}{|\mathbf{u}_i^t \mathbf{v}_i|} \sim \frac{\|\delta \mathbf{I}_N\|_2}{\|\mathbf{v}_i\|_2} \quad (6)$$

where $\|\cdot\|_2$ is the matrix 2-norm [21] and $|\cdot|$ is the standard Euclidean vector norm; \mathbf{u}_i is the left eigenvector of $\langle \hat{\mathbf{I}} \rangle_N$ associated with $\hat{\lambda}_i(N)$. Note that the moment of inertia matrices $\langle \mathbf{I} \rangle_N$ considered here are *symmetric* by definition and therefore the estimates $\mathbf{u}_i^t = \mathbf{v}_i$, at least for sufficiently large N .

To obtain local estimates of ν_i around each walk length N , denoted by $\hat{\nu}_i(N)$, we first took logarithms on both sides in equation (4) to get

$$\log \lambda_i(N) \sim \log A_i + 2\hat{\nu}_i(N) \log N \quad (7)$$

and performed least-square regressions within each window of three data points, $\{(\log k, \log \lambda_i(k)) : k = N/4, N/2, N\}$. Of the three eigenvalues, we focused on the largest and the smallest eigenvalues, as denoted by $\lambda_+(N)$ and $\lambda_-(N)$ and their corresponding size exponents by ν_+ and ν_- , respectively.

Using these local estimates $\hat{\nu}_i(N)$, we then needed to extrapolate to large N using some assumption about possible corrections to scaling. In this way we obtained our final estimate of ν_i , which we denote by $\hat{\nu}_i$. In general, we expect that

$$\hat{\nu}_i(N) \sim \hat{\nu}_i + K N^{-\Delta} \quad (8)$$

with some constants K and $\Delta > 0$. However, the value of Δ , in particular as to whether $\Delta < 1$ in the unrestricted walk model, has been of some debate. For a summary of the history of this debate, refer to Hughes [22]. Recently, due to advances in numerical studies [9] and renormalization group theory [23], it is generally accepted that Δ is in the neighbourhood of $1/2$. Hence, we assumed that $\Delta = 1/2$. For want of better theoretical justification we extrapolated our local estimates using a scale of \sqrt{N} in each TSRW model. The data appeared consistent with this assumption for at least $\hat{\nu}_+(N)$: when we plotted $\hat{\nu}_+(N)$ in each model

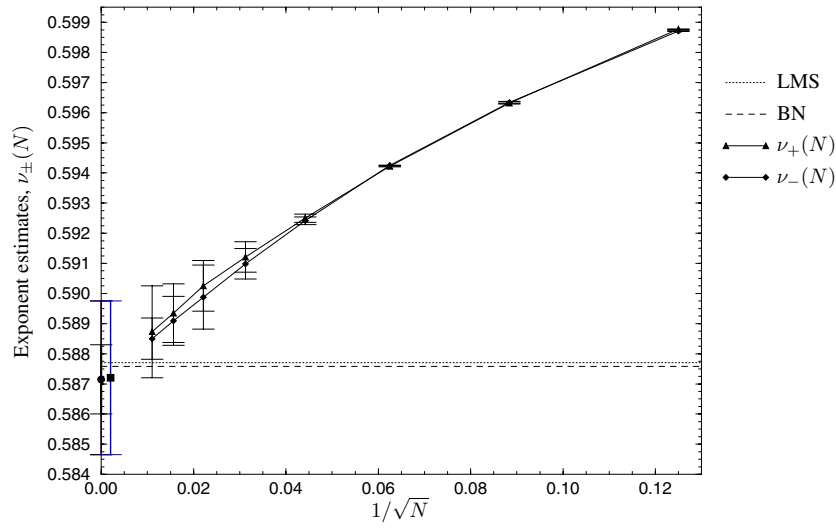


Figure 3. A plot of $\nu_{\pm}(N)$ estimates against $1/\sqrt{N}$ for the unrestricted SAW model. The confidence intervals on the y -axis denote the final estimates of ν_+ (square) and ν_- (circle). (BN and LMS denote the previous ν estimates by Belohorec and Nickel [10] and Li *et al* [9].)

against $1/\sqrt{N}$, fairly straight lines were observed in the asymptotic region in each case, except perhaps for $(P-P-3)$. To obtain the final estimates $\hat{\nu}_{\pm}$ we performed a least-square regression on the plot of $\hat{\nu}_{\pm}(N)$ against $1/\sqrt{N}$ using on the last three or four local estimates.

To benchmark our Monte Carlo simulations, we studied the unrestricted SAW model, $(S-S-S)$. Figure 3 displays a plot of the local exponent estimates $\hat{\nu}_{\pm}(N)$. After extrapolation we have estimated that

$$\hat{\nu}_+ = 0.5874 \pm 0.0033 \tag{9}$$

and

$$\hat{\nu}_- = 0.58715 \pm 0.00150 \tag{10}$$

using a least-square fit on the last three data points. Our estimates are in good agreement with all the earlier estimates as tabulated in table 3. One thing to note in table 3 is that ν estimates are still seemingly affected by some finite-size effects: in general, the ν estimates tend to decrease with the maximum length of the study. Most recent Monte Carlo simulations have focused on very long walks, with one exception by Belohorec and Nickel [10], whose alternative approach [29] analyses very high statistical precision data generated from long runs of short walks. Our simulation data concern moderate to long walks in the context of the studies in table 3.

Additionally, we note that the moment of inertia tensor matrix has the following theoretical form:

$$\langle \mathbf{I} \rangle_N = \begin{pmatrix} a(N) & 0 & 0 \\ 0 & a(N) & 0 \\ 0 & 0 & a(N) \end{pmatrix} \tag{11}$$

where $a(N)$ is some function depending on N . So, this suggests an alternative approach. Perform a *biased* analysis by first forcing the moment of inertia matrix $\langle \hat{\mathbf{I}} \rangle_N$ estimated to adopt such a form. We do this by forcing the off-diagonal entries of $\langle \hat{\mathbf{I}} \rangle_N$ to zero and averaging the diagonal entries of $\langle \hat{\mathbf{I}} \rangle_N$, replacing each entry with this mean value. This procedure also has

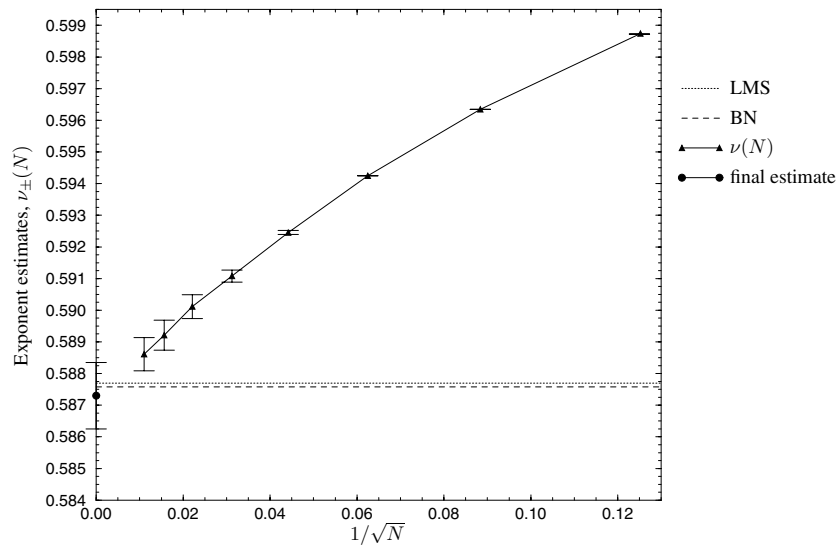


Figure 4. A plot of $\hat{\nu}(N)$ for the unrestricted SAW model.

Table 3. A table summarizing important previous ν estimates for the unrestricted SAW model to-date in chronological order. (N : length of SAWs used in analysis; MC: Monte Carlo; SE: series extrapolation; sc: the simple cubic lattice; bcc: body-centre cubic lattice; d: diamond lattice.)

Source	ν estimate	method
Rapaport [24]	0.592 ± 0.002	MC, $N \leq 2400$ (sc and bcc)
Madras and Sokal [18]	0.592 ± 0.002	MC, $N \leq 3000$ (sc)
Eizenberg and Klafter [25]	0.5909 ± 0.0003	MC, $N \leq 7168$ (sc)
Li <i>et al</i> [9]	0.5877 ± 0.0006	MC, $N \leq 80\,000$ (sc)
Belohorec and Nickel [10]	0.58758 ± 0.00007	MC, $N \leq 384$ (sc)
Prellberg [11]	0.5874 ± 0.0002	MC, $N \leq 16\,384$ (sc)
This work	0.5873 ± 0.0011	MC, $N \leq 8192$ (sc)
Guttmann [26]	0.592 ± 0.003	SE, $N \leq 21$ (sc), 16 (bcc) and 27 (d)
MacDonald <i>et al</i> [27]	0.5875–0.5882	SE, $N \leq 26$ (sc)
Flory [1]	$3/5 = 0.6$	‘Flory argument’
Cotton [28]	0.588 ± 0.002	Light-scattering experiments
Le Guillou and Zinn-Justin [23]	0.588 ± 0.0015	RG, $n = 0$ field theory

the effect of reducing the error bars of each diagonal entry by roughly a factor of $1/\sqrt{3}$. We denote the resulting matrix by $\hat{\mathbf{I}}_N^b$. A plot of exponent estimates $\hat{\nu}(N)$ is shown in figure 4. The final *biased* estimate is

$$\hat{\nu} = 0.5873 \pm 0.0011 \quad (12)$$

where we have used the least-square fit to the last four data points. Again, we note that this estimate is in good agreement with all earlier ν estimates. The sequence $\{\hat{\nu}(N)\}$ appears to behave better than the unbiased counterparts ($\{\hat{\nu}_+(N)\}$ and $\{\hat{\nu}_-(N)\}$), therefore we shall use this estimate as the size exponent estimate for the unrestricted SAW model in subsequent discussion.

Next, we present the results for the four other TSRW models. Let us first consider the (P – P – P) model. We have calculated the local and the final size exponent estimates as we

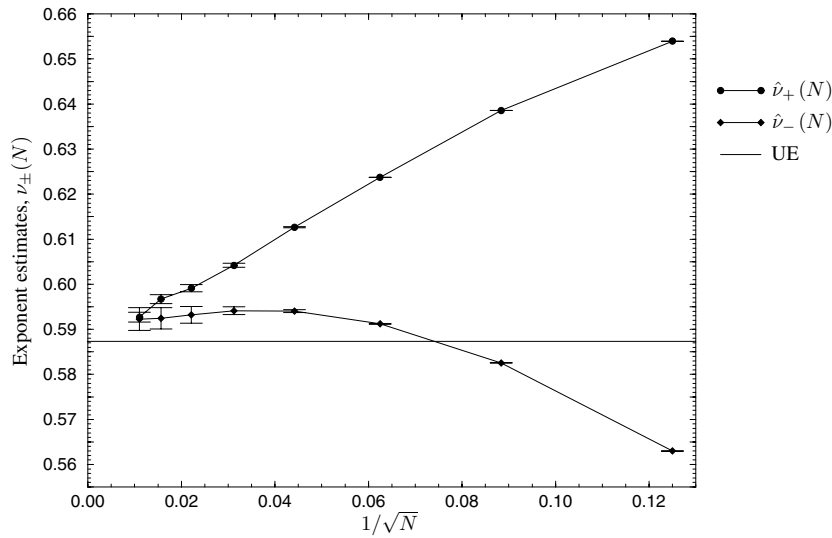


Figure 5. A plot of $\hat{\nu}_{\pm}(N)$ for the $(P-P-P)$ model. UE is the unrestricted ν estimate.

have for the unrestricted model—a plot can be found in figure 5 of the local estimates against $N^{-1/2}$. The final estimates, following extrapolation as above are

$$\hat{\nu}_+ = 0.5873 \pm 0.0027 \tag{13}$$

and

$$\hat{\nu}_- = 0.5910 \pm 0.0047. \tag{14}$$

Both of these final estimates overlap with our ν estimates in the unrestricted model as quoted above. We observe that the above estimate of $\hat{\nu}_-$ is greater than that of $\hat{\nu}_+$ despite $\hat{\nu}_+(N) > \hat{\nu}_-(N)$ as one might expect. This is due to the non-monotonic nature of the corrections to scaling in $\hat{\nu}_-$. (Further details can be found in [30].)

We also note in passing that the theoretical form of the moment of inertia matrices in each TSRW model has some symmetry that we can exploit in order to obtain *biased* estimates (similar to how we have constructed $\langle \mathbf{I} \rangle_N^b$ in the unrestricted model). In doing this we obtained similar central estimates to those catalogued below, albeit with smaller error estimates.

In figure 6 there is a plot of $\hat{\nu}_+(N)$ for the five models considered. The local estimates clearly seem to be tending to a common value. Extrapolations, as described above for the unrestricted model for both $\hat{\nu}_+$ and $\hat{\nu}_-$ are presented in table 4. We note immediately that the central estimates for $\hat{\nu}_-$ are slightly larger than those for $\hat{\nu}_+$ for all the models which implies corrections to scaling still affect some of the estimates, as discussed above for $(P-P-P)$. The estimates $\hat{\nu}_+$ have smaller confidence intervals and are likely to be more reliable. Nevertheless, we observe though that for each of the models the confidence intervals for $\hat{\nu}_-$ overlap with those of $\hat{\nu}_+$, which suggests that $\hat{\nu}_+ = \hat{\nu}_-$ and so that each of the models is *isotropic*.

All estimates of the size exponents confidence intervals reported in each model overlaps with the exponent estimate intervals in the unrestricted SAW model. In fact, the central estimates of $\hat{\nu}_+$ are within 0.0003 of each other at worst, which is a good deal smaller than the confidence intervals quoted. (This may be because the confidence intervals calculated from the simulations are quite conservative.) Therefore, there is no significant difference between size exponents in each restricted model and those of the unrestricted model. As a result,

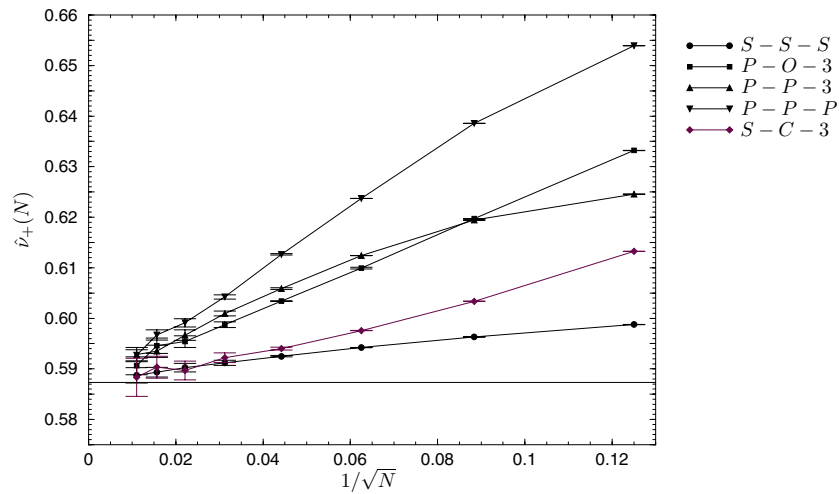


Figure 6. A plot of local estimates of $\hat{\nu}_+(N)$ in all five models, which shows distinct finite-size effects consistent with the series analysis results in [7]. The straight line denotes the size exponent estimate of the unrestricted SAW model.

Table 4. A summary of $\hat{\nu}$ estimates in the five TSRW models. The $(S-S-S)$ estimate quoted is our *biased* estimate.

Model	$\hat{\nu}_+$	$\hat{\nu}_-$
$(P-P-P)$	0.5873 ± 0.0021	0.5910 ± 0.0047
$(S-C-3)$	0.5874 ± 0.0055	0.5896 ± 0.0110
$(P-P-3)$	0.5876 ± 0.0035	0.5893 ± 0.0045
$(P-O-3)$	0.5875 ± 0.0044	0.5894 ± 0.0146
$(S-S-S)$	0.5873 ± 0.0011	0.5873 ± 0.0011

we conclude immediately that *all* non-trivial TSRW models fall into the *same* universality class as the unrestricted SAW, albeit with different corrections to scaling.

4. Discussion

We inferred above that all models studied lie in the same universality class which includes unrestricted SAW. Hence we conclude that all non-trivial TSRW models in three dimensions that are not directed or lower-dimensional in nature lie in the universality class of unrestricted SAW. We can reconcile our conclusion here and the prior delineation of universality class in [7] by noting the various finite-size scaling effects in each model. We refer back to figure 6 for a plot of $\hat{\nu}_+(N)$ for all five models. In the classification in [7], the $(S-C-3)$ model falls into the same class as unrestricted SAW, this is due to the rather *weak* finite-size effect (its line is the closest line to the $(S-S-S)$ line in figure 6). On the other and, it was suggested in [7] that the $(P-P-P)$ model may constitute a distinct universality class, this can be explained by the *strong* finite-size effect (its line is the furthest line from the $(S-S-S)$ line in figure 6). All the other pseudo-universality classes as delineated in [7] can be explained in a similar manner. We note that the systematic error estimate proposed in [7] for differential approximant analyses seems to be a good measure in these models and builds confidence that it may be used more widely in the future.

Table 5. A classification of all TSRW models in three dimensions. The ‘two-dimensional’ class is as per two-dimensional classifications in table 1.

Universality class	ν_+	ν_-
SAW	≈ 0.5873	≈ 0.5873
Directed	1	$\frac{1}{2}$
Two-dimensional	–	–
One-dimensional	1	0 or 1
Zero-dimensional	0	0

In view of this compelling numerical evidence, we give the classification of TSRW models in three dimensions in table 5. There is no overall relationship between the symmetry of walk rules of a model and the universality class into which they fall. The only relevant factor is whether they satisfy the symmetry-mixing conditions. A similar ‘spiral’ class as occurs in two dimensions is apparently missing in three dimensions, which suggests that the two-dimensional spiral walk is a unique product of both the walk rule and the specific topology of two-dimensional lattices. In three dimensions spirality cannot be enforced by placing two-step restrictions since a growing walk can always escape around the walk already in existence so breaking strict spirality.

Acknowledgments

We thank A Rechnitzer for giving us valuable comments on the manuscripts. LHW thanks The University of Melbourne for a Melbourne Research Scholarship and the David Hay Postgraduate Write-up Award. Financial support from the Australian Research Council is gratefully acknowledged by ALO.

References

- [1] Flory P J 1971 *Principles of Polymer Chemistry* (New York: Cornell University Press)
- [2] de Gennes P-G 1979 *Scaling Concepts in Polymer Physics* (New York: Cornell University Press)
- [3] Madras N and Slade G 1993 *The Self-avoiding Walks* (Cambridge, MA: Birkhäuser Boston)
- [4] Vanderzande C 1998 *Lattice Model of Polymers* (Cambridge: Cambridge University Press)
- [5] Guttmann A J 2000 Indicators of solvability for lattice models *Disc. Math.* **217** 167–89
- [6] Guttmann A J, Prellberg T and Owczarek A L 1993 On the symmetry classes of planar self-avoiding walks *J. Phys. A: Math. Gen.* **26** 6615–23
- [7] Rechnitzer A D and Owczarek A L 2000 On the three-dimensional self-avoiding walk symmetry classes *J. Phys. A: Math. Gen.* **33** 2685–723
- [8] Nienhuis B 1982 Exact critical point and critical exponents of $O(n)$ model in two dimensions *Phys. Rev. Lett.* **49** 1062–5
- [9] Li B, Madras N and Sokal A L 1995 Critical exponent, hyper-scaling, and universal amplitude ratios for two- and three-dimensional self-avoiding walks *J. Stat. Phys.* **80** 661–754
- [10] Belohorec P and Nickel B 1997 University of Guelph *Preprint*
- [11] Prellberg T 2001 Scaling of self-avoiding walks and self-avoiding trails in three dimensions *J. Phys. A: Math. Gen.* **34** L599–L602
- [12] Janse van Rensburg E J 2000 *The Statistical Mechanics of Interacting Walks, Polygons, Animals and Vesicles* (Oxford: Oxford University Press)
- [13] Owczarek A L, Rechnitzer A D and Wong L H 2001 Addendum to ‘On the three-dimensional self-avoiding walk symmetry classes’ *J. Phys. A: Math. Gen.* **34** 6055–60
- [14] Brak R, Owczarek A L and Soteros C E 1998 On anisotropic spiral self-avoiding walks *J. Phys. A: Math. Gen.* **31** 4851–69

-
- [15] Guttmann A J and Wallace K J 1985 On three-dimensional spiral anisotropic self-avoiding walks *J. Phys. A: Math. Gen.* **18** L1049–L1054
 - [16] Guttmann A J 1989 Asymptotic analysis of power series expansions *Phase Transitions and Critical Phenomena* vol 13, ed C Domb and J L Lebowitz (New York: Academic)
 - [17] Grassberger P 1997 Pruned-enriched Rosenbluth method: simulation of θ polymer of chain length up to 1 000 000 *Phys. Rev. E* **56** 3682–93
 - [18] Madras N and Sokal A D 1988 The pivot algorithm: a highly efficient Monte Carlo algorithm for the self-avoiding walks *J. Stat. Phys.* **50** 109–86
 - [19] Prellberg T and Owczarek A L 2000 Four-dimensional polymer collapse: pseudo-first-order transition in interacting self-avoiding walks *Phys. Rev. E* **62** 3780–9
 - [20] Wilkinson J H 1965 *The Algebraic Eigenvalue Problem* (Oxford: Oxford University Press)
 - [21] Bhatia R 1997 *Matrix Analysis* (New York: Springer)
 - [22] Hughes B D 1995 *Random Walks and Random Environments* vol 1 (London: Clarendon)
 - [23] Le Guillou J C and Zinn-Justin J 1980 Critical exponents from field theory *Phys. Rev. B* **21** 3976–98
 - [24] Rapport D C 1985 On three-dimensional self-avoiding walk *J. Phys. A: Math. Gen.* **18** 113–26
 - [25] Eizenberg N and Klafter J 1993 Self-avoiding walks on a simple cubic lattice *J. Chem. Phys.* **99** 3976–82
 - [26] Guttmann A J 1987 On the critical behaviours of self-avoiding walks *J. Phys. A: Math. Gen.* **20** 1839–54
 - [27] MacDonald D, Joseph S, Hunter D L, Moseley L L, Jan N and Guttmann A J 2000 Self-avoiding walks on the simple cubic lattice *J. Phys. A: Math. Gen.* **33** 5973–83
 - [28] Cotton J P 1980 Polymer excluded volume exponent—an experimental verification of the N -vector model for $N = 0$ *J. Physique Lett. (Paris)* **41** L231–4
 - [29] Nickel B 2003 Private communication
 - [30] Wong L H 2003 Topics on lattice models in statistical mechanics *PhD Thesis* The University of Melbourne